

Lifetime of photogenerated carriers in silicon-on-insulator rib waveguides

D. Dimitropoulos, R. Jhaveri, R. Claps, J. C. S. Woo, and B. Jalali^{a)}
 University of California, Los Angeles, Department of Electrical Engineering,
 Los Angeles, California 90095-1594

(Received 2 August 2004; accepted 14 January 2005; published online 10 February 2005)

The lifetime of photogenerated carriers in silicon-on-insulator rib waveguides is studied in connection with the optical loss they produce via nonlinear absorption. We present an analytical model as well as two-dimensional numerical simulation of carrier transport to elucidate the dependence of the carrier density on the geometrical features of the waveguide. The results suggest that effective carrier lifetimes of ≤ 1 ns can be obtained in submicron waveguides resulting in negligible nonlinear absorption. It is also shown that the lifetime and, hence, carrier density can be further reduced by application of a reverse bias *pn* junction. © 2005 American Institute of Physics. [DOI: 10.1063/1.1866635]

Silicon integrated optics has emerged as an attractive technology for realizing passive devices because of the efficient silicon-on-insulator (SOI) guiding structures and foundry compatible processing technology. Recently nonlinear optical processes have been observed in SOI waveguides under high optical intensities at telecom wavelengths,¹⁻⁵ highlighting the potential for active devices that rely on the nonlinear optical response. Although silicon has negligible optical absorption around this wavelength, at high optical intensities, optical absorption and consequently photogeneration can occur due to two-photon absorption (TPA).^{6,7} Under steady state illumination the carrier density can reach values as high as $\sim 10^{18}$ cm⁻³ and cause significant optical loss, which prohibits the exploitation of useful optical nonlinearities. Since the steady state carrier density is proportional to the lifetime, the latter represents the critical parameter that will determine the magnitude of free carrier absorption at a given optical intensity. In this letter, we study the carrier lifetime in silicon rib waveguides and its dependence on lateral waveguide dimension. We present a simple analytical expression for the lifetime which includes carrier recombination at the Si/SiO₂ interface and at the silicon surface, as well as carrier diffusion. The model shows excellent agreement with two-dimensional numerical simulations and provides a convenient tool for calculating the TPA induced free carrier losses in silicon waveguides. We also study the effectiveness of a reverse biased *pn* junction in sweeping out the photogenerated carriers in waveguides with various dimensions.

To quantify the carrier density we performed simulations with a commercial software (ATLAS, ATHENA v. 5.6.0.R Silvaco International). The geometry of a rib waveguide that we analyzed is shown in Fig. 1. These structures can be either single-mode or multimode depending on the ratio of the dimensions w/H and h/H .⁸ In all cases we consider the optical intensity to propagate in the lowest order TE mode. The two-photon absorption process results in an intensity dependent loss of the form $dI/dz = -\beta I^2$, where z denotes distance in the waveguide and I is the optical intensity. The constant β is called the two-photon absorption frequency coefficient and depends on the material and the optical frequency. For

silicon $\beta \sim 7 \times 10^{-10}$ cm/W.^{9,4,1} For every photon pair that is absorbed an electron-hole pair is generated so that if N (units of cm⁻³) is the electron density, then the generation rate is $G = dN/dt = -(1/2E)dI/dz = (1/2E)\beta I^2$, where E is the photon energy. The mode of the rib waveguide has a nonuniform transversal distribution and thus the generation rate itself is nonuniform over the waveguide cross section. To model this effect we used Gaussian distribution of the optical intensity (which highly resembles the mode profile) with a half-width that matched the actual mode profile. The peak of the distribution is chosen so that the integral of the distribution along the transverse dimensions equals $G \times wH$ ($G = 10^{25}$ cm⁻³ s⁻¹). We define an effective lifetime to characterize the carrier density as $\tau_{\text{eff}} = N/G$, where N is the carrier density. Once the carrier density is known the optical dispersion and loss are readily determined,¹⁰ e.g., at 1.55 μm the loss is $\alpha(\text{cm}^{-1}) = 1.45 \times 10^{-17} \times N(\text{cm}^{-3})$.

The processes that balance the carrier generation and hence determine the carrier density are (i) diffusion and (ii) recombination at traps at the Si-SiO₂ interface and at the silicon surface. Because the rib width is much smaller than the diffusion length we expect the carrier distribution to be approximately uniform under the rib. This is a very good approximation for all the cases studied in this letter and permits us to derive an analytical expression for the effective lifetime.

In steady state ($\partial n/\partial t = 0$) the two-dimensional continuity equation is

$$\oint \mathbf{f} \cdot \hat{\rho} dl = \int (G - n/\tau_b) dA. \quad (1)$$

Here, $\hat{\rho}$ is a vector perpendicular to the path of integration, dl and dA are differentials of the contour length and area, respectively, G is the generation rate and τ_b is the bulk

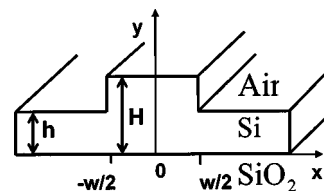


FIG. 1. Rib waveguide geometry.

^{a)}Electronic mail: jalali@ucla.edu

recombination lifetime. In the bulk, $\mathbf{f} = -D\nabla n$, whereas at the Si/SiO₂ interface, $\mathbf{f} \cdot \hat{\rho} = Sn$, where S is the interface recombination velocity. Similarly for the silicon surface $\mathbf{f} \cdot \hat{\rho} = S'n$, where S' is the surface recombination velocity. If we evaluate the continuity equation for the rib area we obtain

$$wH \left(G - \frac{n}{\tau_b} \right) = -2hD \frac{dn}{dx} + wSn + [w + 2(H-h)]S'n. \quad (2)$$

Outside the rib ($x > w/2$) the carrier density has the form

$$n(x) = n(w/2) \exp[-(x - w/2)/L'], \quad (3)$$

where $L' = \sqrt{D\tau'}$ is the diffusion length and $1/\tau' = 1/\tau_b + (S+S')/h$. Using Eqs. (2) and (3) we can obtain an expression for the effective lifetime in the waveguide

$$\frac{1}{\tau_{\text{eff}}} = \frac{G}{n} = \frac{1}{\tau_b} + \frac{S}{H} + \frac{w + 2(H-h)}{wH} S' + 2 \frac{h}{H} \sqrt{\frac{D}{w^2} \left(\frac{1}{\tau_b} + \frac{S+S'}{h} \right)}. \quad (4)$$

In the earlier equation, both the diffusion coefficient and the interface recombination velocity are dependent upon the carrier densities and the latter is given by a Read-Shockley type expression.¹¹ For high injection conditions where the generated carrier density is above the doping level, the ambipolar diffusion coefficient must be used.¹² Similarly if S is the minority carrier interface recombination velocity, the Read-Shockley expression gives an effective interface recombination velocity $\approx S/2$ under high injection levels.¹¹

Another effect that results in the dependence of lifetime on carrier density is the Auger effect. The Auger recombination rate has the form $R_A = Fn^3$ and for silicon F is between 3×10^{-31} and 10^{-30} cm⁶/s.¹³ This recombination rate is significant when it is of the same order of magnitude as the generation rate. This happens when $G \sim Fn^3$ which gives $n \sim 3 \times 10^{18}$ cm⁻³. When G and n have these values the effective lifetime is 300 ns. As long as $n \ll 3 \times 10^{18}$ cm⁻³ or $\tau_{\text{eff}} \ll 300$ ns the Auger term is negligible. While the analytical model does not include the Auger effect, the effect is included in the numerical simulations.

In many cases of practical interest the surface recombination is negligible when compared to the recombination at the interface. High quality passivated surfaces have surface recombination velocities of the order of tens of cm/s whereas when the surface is not treated recombination velocities can be several thousand cm/s.¹⁴ On the other hand, interface recombination velocities between 10^3 and 10^4 cm/s are common in the Si/SiO₂ interface.¹⁵

In both the numerical simulations and the analytical model, we use mobility values of $\mu_e = 1332$ cm² V⁻¹ s⁻¹, $\mu_h = 455$ cm² V⁻¹ s⁻¹ (these values correspond to doping density $\sim 2 \times 10^{15}$ cm⁻³), bulk recombination lifetimes $\tau_{\text{bc}} = 3$ μ s, $\tau_{\text{bh}} = 10$ μ s, and interface recombination velocity $S = 8 \times 10^3$ cm/s. As stated earlier we assume high quality waveguide surfaces such that the surface recombination velocity is negligible.

We first simulated the dependence of the lifetime on the ratio of slab height to rib height (h/H) with the constraint $w = H$. The lifetime is computed for different values of H . The results of numerical simulations are shown in Fig. 2 along with the same predicted by the analytical model de-

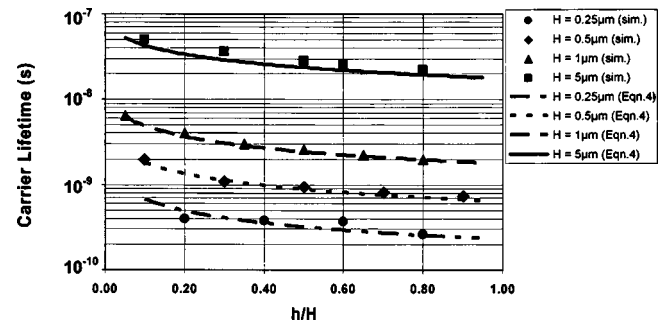


FIG. 2. Dependence of the effective carrier lifetime over the ratio h/H for $H = 0.25, 0.5, 1, \text{ and } 5 \mu\text{m}$ ($w/H = 1$ in all cases). Both simulated results and the predictions of Eq. (4) are also shown.

scribed by Eq. (4). We note that as H is reduced towards submicron dimensions the recombination at the interface becomes more effective and the lifetime is reduced. For a given height H the lifetime decreases as h increases, since the carriers can diffuse more effectively away from the waveguide core and into the surrounding slab regions (assuming the surface recombination can be neglected). For submicron waveguides with $w = H = 0.5 \mu\text{m}$, lifetime is around 1 ns.

The explicit dependence of lifetime on waveguide width is summarized in Fig. 3. Here, the rib height is kept to constant values of $H = 5 \mu\text{m}$ and $H = 0.5 \mu\text{m}$. As w decreases the lifetime decreases. This behavior comes about because when w becomes smaller the transit time for the carriers to diffuse out of the rib region decreases.

The model predicts a reduction of effective lifetime with scaling of waveguide cross section, a welcoming trend as it lowers TPA induced free carrier loss. As an example, if we consider a channel waveguide with $w = 450$ nm and $H = 250$ nm with unpassivated surfaces such that $S = S' = 8000$ cm/s, the model predicts an effective lifetime of 1 ns. For such dimensions, both Almeida *et al.*¹⁶ and Espinola *et al.*¹⁷ have reported lifetimes on the order of 1 ns.

To achieve even lower densities an electric field will have to be introduced to sweep the carriers out. A similar approach has been effectively used to reduce the effective lifetime in saturable absorbers.¹⁸ A $p-i-n$ junction can be formed by placing $n+$ and $p+$ junctions in the slab region surrounding the rib, with the resulting structure resembling the commercially available silicon variable optical attenuators.¹⁹ Dopant densities of 10^{18} cm⁻³ can create considerable built-in junction field intensities in submicron waveguides. The doped regions must be far enough from the rib so it does not have significant overlap with the optical

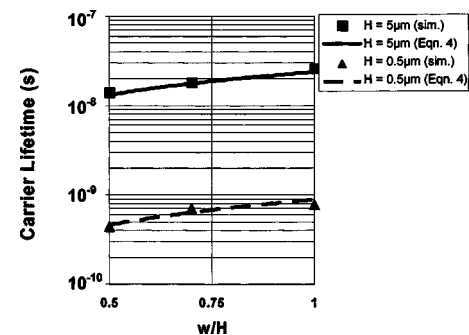


FIG. 3. Dependence of the effective carrier lifetime over the rib width ($h = 0.6H$, $H = 5 \mu\text{m}$). Both simulated results and the predictions of Eq. (4) are also shown.

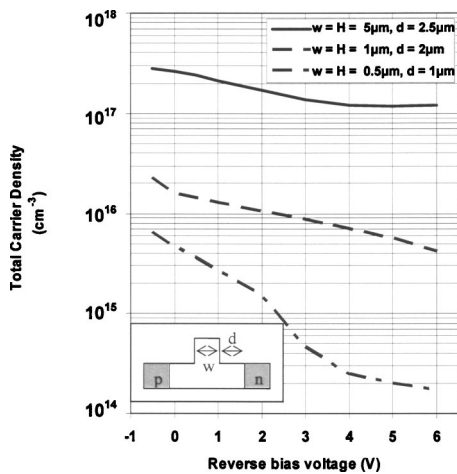


FIG. 4. Simulated results for the dependence of the total carrier density on the reverse applied voltage. The average generation rate is $10^{25} \text{ cm}^{-3} \text{ s}^{-1}$.

mode and, hence, optical losses are kept low. On the other hand, they must be close enough so that the built-in field depletes the rib of free carriers. In Fig. 4 simulated results are shown for waveguides with $h=0.5H$, and $w=H=0.5, 1$, and $5 \mu\text{m}$. For smaller rib dimensions, the mode is smaller, hence, the $p+$ and $n+$ regions can be placed closer to the rib. With this in mind, the distances of the edges of the $p-$ and $n-$ doped regions from the rib for these examples, were chosen to be 1, 2, and $2.5 \mu\text{m}$, respectively. For these values, the optical losses resulting from the highly doped regions were simulated with commercial software (FIMMWAVE v 4.1.6, Photon Design) to be less than 0.02 dB/cm . As the results show rib dimensions and the distance from the rib drastically affect the carrier sweep out. For widths of the order of $0.5 \mu\text{m}$ the junction is very effective in reducing the total carrier density below $5 \times 10^{15} \text{ cm}^{-3}$ and ensure negligible extra losses. The price for the low lifetime is a high current at the junction electrodes. For a 0.5 cm long waveguide, simulations suggest a reverse current of $50\text{--}250 \text{ mA}$.

In conclusion we have investigated the carrier lifetime of photogenerated carriers in SOI waveguides. As the wave-

guide lateral dimensions are reduced the carrier density decreases significantly. This is due to the carrier recombination at the Si-SiO_2 interface, which becomes more effective as the rib height is decreased, as well as lateral diffusion into the slab regions surrounding the rib. Further decrease of the carrier density can be achieved by introducing an electric field by means of a $p-i-n$ junction along the waveguide.

This work was supported by the MTO office of the Defense Advance Research Project Agency (DARPA). The authors would like to thank Dr. Jag Shah for his support.

- ¹R. Claps, D. Dimitropoulos, V. Raghunathan, Y. Han, and B. Jalali, *Opt. Express* **11**, 1731 (2003).
- ²R. Claps, V. Raghunathan, D. Dimitropoulos, and B. Jalali, *Opt. Express* **11**, 2862 (2003).
- ³D. Dimitropoulos, V. Raghunathan, and R. Claps, *Opt. Express* **12**, 149 (2004).
- ⁴H. K. Tsang, C. S. Wong, T. K. Liang, I. E. Day, S. W. Roberts, A. Harpin, J. Drake, and M. Asghari, *Appl. Phys. Lett.* **80**, 416 (2002).
- ⁵J. I. Dadap, R. L. Espinola, and R. M. Osgood, Jr., *Integrated Photonics Research Conference (IPR) 2004 IWA4*, 2004, Vol. 27, p. 1971.
- ⁶T. K. Liang and H. K. Tsang, *Appl. Phys. Lett.* **82**, 2745 (2004).
- ⁷R. Claps, V. Raghunathan, D. Dimitropoulos, and B. Jalali, *Opt. Express* **12**, 2774 (2004).
- ⁸R. A. Soref, J. Schmidtchen, and K. Petermann, *IEEE J. Quantum Electron.* **27**, 1971 (2004).
- ⁹J. F. Reintjes and J. C. McGroddy, *Phys. Rev. Lett.* **30**, 901 (1973).
- ¹⁰R. A. Soref and B. R. Bennett, *IEEE J. Quantum Electron.* **QE-23**, 123 (1987).
- ¹¹S. M. Sze, *Physics of Semiconductor Devices*, 2nd ed. (Wiley, New York, 1981), p. 35.
- ¹²K. Seeger, *Semiconductor Physics*, 3rd ed. (Springer, Berlin, 1985), p. 117.
- ¹³M. J. Kerr and A. Cuevas, *J. Appl. Phys.* **91**, 2473 (2002).
- ¹⁴O. Palais and A. Arcari, *J. Appl. Phys.* **93**, 4686 (2003).
- ¹⁵T. Kuwayama, M. Ichimura, and E. Arai, *Appl. Phys. Lett.* **83**, 928 (2003).
- ¹⁶V. R. Almeida, C. A. Barrios, R. R. Panepucci, M. Lipson, M. A. Foster, D. G. Ouzounov, and A. L. Gaeta, *CLEO 2004 CTuFF3*.
- ¹⁷R. L. Espinola, J. I. Dadap, R. M. Osgood, Jr., S. J. McNab, and Y. A. Vlasov, *Opt. Express* **12**, 3713 (2004).
- ¹⁸E. P. Burr, J. B. Song, A. J. Seeds, and C. C. Button, *J. Appl. Phys.* **90**, 3566 (2001).
- ¹⁹R. R. Whiteman, A. P. Knights, D. George, I. E. Day, A. Vonsovici, A. A. House, G. F. Hopper, and M. Asghari, *Proc. SPIE* **4997**, 146 (2003).